UDK 544.6:544.52:620.3
Original scientific article/Izvirni znanstveni članek

ISSN 1580-2949
MTAEC9, 52(4)397(2018)

PREPARATION AND PHOTO-ELECTROCHEMICAL PERFORMANCE OF TiO_2 NANOTUBE ARRAYS FOR WATER SPLITTING MODIFIED WITH CuO VIA A SIMPLE METHOD

ENOSTAVNA METODA PRIPRAVE MNOŽICE S CuO MODIFICIRANIH TIO_2 NANOCEVK ZA POSTOPEK RAZCEPLJANJA VODE TER NJIHOVE FOTOELEKTROKEMIČNE LASTNOSTI

Hongxing Dong[1], Qiuping Liu[2], Yuehui He[3]

[1]College of Electromechanical Engineering, Hangzhou Polytechnic, Hangzhou, Zhejiang, China
[2]College of Chemical Engineering, Zhejiang University of Technology, Hangzhou, Zhejiang, China
[3]State Key Laboratory of Powder Metallurgy, Central South University, Changsha 410083, China
liuqiuping@zjut.edu.cn

Prejem rokopisa – received: 2017-08-22; sprejem za objavo – accepted for publication: 2018-01-09

doi:10.17222/mit.2017.138

A CuO/TiO_2/Ti heterojunction photo-electrode was fabricated based on TiO_2 nanotube arrays, prepared with anodic oxidation. A facile and economical wet impregnation followed by annealing was employed to fabricate CuO-modified TiO_2 nanotube arrays. The structural and optical properties were characterized with SEM, EDX, XRD and UV-Vis spectrometry. The photo-electrochemical properties were measured with CHI 660E under a 150WXe lamp and in the dark. Moderate amounts of the CuO-modified TiO_2 nanotube arrays (TiO_2-CuO (I)) exhibited photocurrents of 4.633×10^{-5}A/cm^2 and 2.29×10^{-5}A/cm^2 at –0.35 V (vs. SCE) in a 0.2 M Na_2SO_4 electrolyte under the light and in the dark, respectively. The current density of TiO_2-CuO (I) was higher than that of the pure-TiO_2 electrode in the light, but the current density of TiO_2-CuO (I) was lower than that of pure TiO_2 in the dark. Therefore, the CuO on the TiO_2 surface increased the electrical resistance. Significantly, the CuO films of TiO_2-CuO (II) were too thick to decrease the photo-electrochemical activity, which was confirmed with electrochemical impedance spectroscopy.

Keywords: TiO_2 nanotube arrays, CuO, photo-electrochemistry, water splitting

Avtorji prispevka so večstično CuO/TiO_2/Ti fotoelektrodo izdelali na množici TiO_2 nanocevk, ki so bile izdelane z anodno oksidacijo. Sledila je enostavna in ekonomična izdelava množice s CuO modificiranih TiO_2 nanocevk z mokro impregnacijo, kateri je sledil postopek žarjenja. Avtorji so strukturne in optične lastnosti določili s SEM, EDX, XRD in UV-Vis spektrometrijo. Fotoelektrokemične lastnosti so določili s CHI 660E pod 150WXe žarnico in v temi. Zmerna količina množice s CuO modificiranih TiO_2 nanocevk (TiO_2-CuO (I)) je imela gostoto fotoelektričnega toka $4,633 \times 10^{-5}$ A/cm^2 in $2,29 \times 10^{-5}$ A/cm^2 pri –0.35 V (vs. SCE) v 0,2 M elektrolitu Na_2SO_4 pod lučjo oz. v temi. Gostota toka TiO_2-CuO (I) je višja kot jo ima čista TiO_2 elektroda pod lučjo, toda v temi je gostota TiO_2-CuO (I) nižja kot jo ima čista TiO_2 elektroda v temi. Zato CuO na površini TiO_2 povečuje električno upornost. Pomembna je ugotovitev, da so bili CuO filmi TiO_2-CuO (II) predebeli, da bi se zmanjšala fotoelektrokemična aktivnost, ki so jo avtorji potrdili z elektrokemično impedančno spektroskopijo.

Ključne besede: množica TiO_2 nanocevk, CuO, fotoelektrokemija, razcepljanje vode (ločitev na vodik in kisik)

1 INTRODUCTION

Renewable energy is vital to the development of the world. The application of solar energy for the production of clean oxygen and hydrogen fuels, using photo-electrochemical splitting of water, is a promising way.[1] The usage of metal-oxide semiconductors in the conversion of solar energy to electrical energy has recently attracted more attention due to their chemical stability and environmentally friendly and cost-efficient production methods.[2,3]

Titanium dioxide (TiO_2) is considered to be a favorable photocatalyst due to its relatively cheap, chemically stable high photocatalytic performance and nontoxicity.[4,5] A TiO_2 nanotube exhibits a unique combination of morphological and physicochemical properties, including a high aspect ratio, mesoporous structure and efficient electron conductivity.[3] It was reported that TiO_2 nanotubes have a great potential for the application in the areas including gas sensing, environmental purification and photocatalytic hydrogen production.[3,6,7] The hydrogen-generation efficiency over bare TiO_2 is relatively low because of the fast recombination of electro-hole pairs.[8,9] To overcome the shortcoming, many modification methods have been reported, involving semiconductor composition, metal-ion doping and noble-metal loading.[10–12]

Recently, copper oxide (Cu_2O, Cu^{2+}, CuO, etc.) based TiO_2 composites have been reported to be efficient photocatalysts for water splitting and many other photo-oxidation reactions.[13,14] Copper compounds are good for the charge separation and provide reduction sites for hydrogen formation. Moreover, a surface modification with CuO can widen the absorption of the wave range from 200 nm to 500 nm.[15] The wet-impregnation

(WI) method proved to be an effective way to incorporate semiconductor compositions.[16,17] However, few results showed detailed influence effects of the wet-impregnation methods on the photocatalytic properties. In addition, there are few works focusing on TiO_2 nanotube arrays modified with wet impregnation.

In this paper, TiO_2 nanotube arrays were produced using the anodic oxidation method, and then CuO was incorporated with WI followed by sintering. The photo-electrochemical performance of the resulting CuO-TiO_2 was obtained in the same impregnation liquid with a different treatment. In order to elucidate the influence effects, electrochemical impedance spectroscopy (EIS) was carried out. The influence factors that contribute to the high photo-electrochemical performance were discussed. And the factors influencing the charge transfer in the TiO_2 nanotube arrays modified by CuO were also evaluated. The result will help us to design a new kind of efficient photo-electrode material for water splitting through wet impregnation.

2 EXPERIMENTAL PART

2.1 Synthesis of TiO_2 nanotube arrays

Commercially pure titanium plates (0.5 mm thick, purity > 99.5 %) were first degreased in acetone, then mechanically polished, and finally chemically polished at 25 °C in a solution consisting of H_2O:HNO_3:HF = 6:3:1 (V %) for 30 s. The pretreated titanium plates were anodic oxidized in 1 % mass fraction hydrofluoric-acid solution at 20 V for 30 min to produce TiO_2 nanotube arrays. Then the TiO_2 nanotube arrays were washed with de-ionized water three times and dried for the next step. The prepared TiO_2 nanotube arrays were finally sintered in air at 500 °C for 2 h to prepare sintered TiO_2 nanotube arrays.

2.2 Preparation of TiO_2-CuO photo-electrodes

The CuO-modified TiO_2 nanotube arrays were obtained with WI, followed by sintering. Cu $(NO_3)_2 \cdot 3H_2O$ was used as the Cu^{2+} precursor. 30g Cu $(NO_3)_2 \cdot 3H_2O$ was dispersed into 100 mL of de-ionized water. The as-prepared TiO_2 nanotube arrays were immersed into the Cu $(NO_3)_2$ solution treated with ultrasonic waves for 30 min and then dried in a furnace at 80 °C for 30 min. The obtained sample was denoted as TiO_2-Cu $(NO_3)_2$. TiO_2-CuO (I) was obtained by carefully drip washing TiO_2-Cu $(NO_3)_2$ with de-ionized water to remove the redundant Cu $(NO_3)_2$ followed by sintering at 500 °C for 2h. TiO_2-CuO (II) was obtained by sintering TiO_2-Cu $(NO_3)_2$ in air at 500 °C for 2 h. The fabrication process of the TiO_2-CuO (I) and TiO_2-CuO (II) photo-electrodes is shown in **Figure 1**.

2.3 Characterization

The surface morphology of the sintered TiO_2 nanotube arrays, TiO_2-CuO (I) and TiO_2-CuO (II) was observed with a Hitachi S-4700 field-emission scanning electron microscope (FESEM) after spraying the conducting layer of platinum. The bulk composition was investigated with energy dispersive X-ray spectroscopy (EDS). The phases present in the coatings were characterized with a small-angle diffractometric study carried out on a Riga KUD/max 2550PC X-ray automatic diffractometer. The optical performance was evaluated using an Agilent Technologies Cary 500 spectrophotometer with its wavelength ranging from 200 nm to 800 nm.

The photo-electrochemical performance was evaluated in a three-electrode electrochemical cell with a quartz window to allow illumination. The working electrodes were the sintered TiO_2, TiO_2-CuO (I) and TiO_2-CuO (II). A saturated calomel electrode (SCE) and Pt silk served as the reference electrode and counter electrode, respectively. All the working electrodes were tested in 0.2 M Na_2SO_4 and analyzed with a CHI660E electrochemical analyzer. Linear sweep voltammetry (LSV) was measured at a scan rate of 0.01 VS^{-1}. Electrochemical impedance spectroscopy (EIS) was carried out under an open-circuit voltage with frequencies ranging from 10^5 to 10^{-2} Hz with an AC voltage amplitude of 5 mV. The potentials in the I–V and I–t curves, and in the PEC degradation experiments, were controlled by CHI660E. A 150WXe lamp was used to

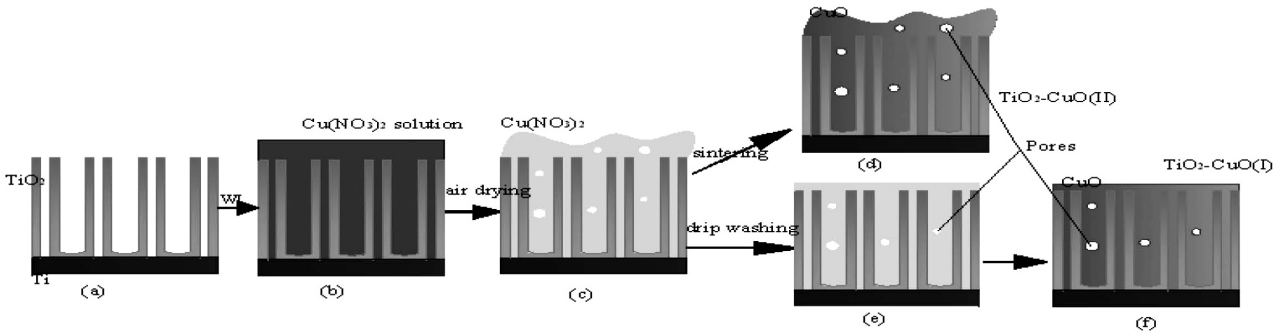

Figure 1: Fabrication process of TiO_2-CuO photo-electrodes: a) TiO_2 nanotube arrays produced with anodic oxidation, b) wet impregnation of the Cu $(NO_3)_2$ solution, c) air drying of sample b at 80 °C for 30 min, d)TiO_2-CuO (II) produced by sintering in air at 500 °C for 2 h, e) drip washing of sample c to remove the redundant $Cu(NO_3)_2$ on the surface, f) TiO_2-CuO (I) produced by sintering sample e in air at 500 °C for 2 h

provide visible light. Electrochemical impedance spectroscopy was used to explore the conductivity of the electrodes under the dark and illumination environment. The solution was the same as that used for the photo-electrochemical-performance evaluation.

3 RESULTS AND DISCUSSION

3.1 SEM analysis

Surface morphology was observed with FESEM. It is found that TiO_2 nanotube arrays are formed having a regular and orderly structure (**Figure 2a**). The average diameter of these nanotubes is around 100 nm and the thickness of a wall is around 20 nm. The length of TiO_2 nanotube arrays is around 200 nm. There is an interstice between TiO_2 nanotubes. H. Zao et al.[18] also reported that there is an interstice between TiO_2 nanotube arrays. The length of the TiO_2 nanotubes is around 200 nm. Porous clusters were found on the TiO_2-CuO (II) surface (**Figure 2b**), and the thickness of a nanosheet is around 100 nm. The top and cross-section images of TiO_2-CuO (I) are shown in **Figures 2c** and **2d**, respectively. The thickness of TiO_2-CuO (I) is around 200 nm. The inset image in **Figure 2d** is the cross-section image of TiO_2-CuO (II), and the thickness of the film is around 3 μm. The energy-dispersive-spectrometer analysis shows that there are Cu (x = 54.5 %), O (x = 36.75 %) and Ti (x = 8.75 %) on the TiO_2-CuO (II) surface, and the Cu amount is much larger than that of Ti, indicating the Cu oxide on the TiO_2 surface is thick. Nanoparticle and porous films were found on the TiO_2-CuO (I) surface. The Cu (x = 28.82 %) amount is almost as big as that of Ti (x = 20.01 %), indicating the Cu oxide on the surface is thinner than that of TiO_2-CuO (II).

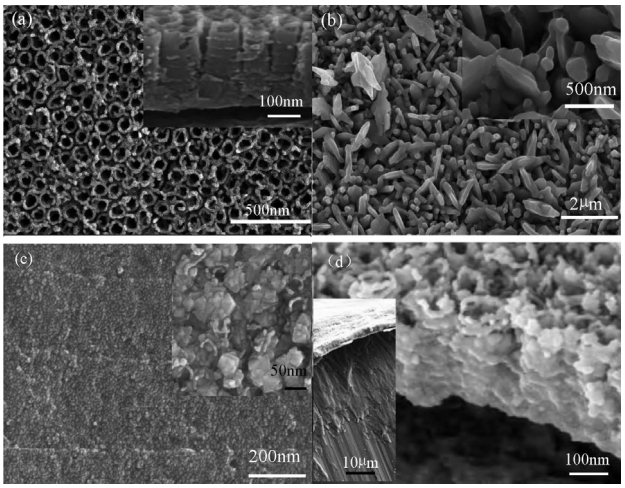

Figure 2: SEM images of the as-prepared photochemical electrodes: a) SEM image of the sintered TiO_2 surface, the inset is the cross-section image, b) SEM images of the TiO_2-CuO (II) surface, c) SEM images of the TiO_2-CuO (I) surface, d) cross-section image of TiO_2-CuO (I), the inset is the cross-section image of TiO_2-CuO (II)

However, the FESEM and EDS analyses do not allow us to distinguish between TiO_2 and Cu oxide. Therefore, other method, i.e., X-ray diffraction was applied.

3.2 XRD analysis

Figure 3 indicates the XRD patterns for the sintered TiO_2 nanotube arrays and CuO-modified TiO_2 nanotube arrays. The major peaks corresponding to the CuO crystallites at 2θ = 35.5° and 38.4° are clearly shown in **Figures 3b** and **3c**. The peak intensity at 2θ = 35.5° and of 38.4° in **Figure 3b** is much stronger than that in **Figure 3c**, indicating that the amount of CuO in TiO_2-CuO (II) is larger than that in TiO_2-CuO (I). The XRD pattern for the CuO on TiO_2 nanotube arrays can be indexed to the monoclinic phase of CuO without Cu and Cu_2O, showing that the CuO nanostructure is well crystallized and pure after being sintered in air at 500 °C. L. Valladares et al.[19] showed that Cu was totally transformed into CuO when the sintering temperature was above 300 °C. All the results demonstrated that CuO was well crystallized on the surface of the TiO_2 nanotube arrays.

The average crystal sizes for CuO with a cell volume of 20.63 nm in TiO_2-CuO (II) are calculated, after an appropriate background correction, from the X-ray line, broadening the diffraction peaks at 2θ = 35.5° and 38.4° using Debye-Scherrer's formula:[20]

$$D=0.89\lambda/\beta\mathrm{Cos}\ \theta \quad (1)$$

where λ is 0.15406 nm (the wave length of the X-ray), β is the angular peak width at half maximum in radians, and θ is Bragg's diffraction angle.

3.3 UV-Vis diffuse-reflectance-spectra analysis

Figure 4 displays the diffuse-reflectance spectra of sintered TiO_2, TiO_2-CuO (I) and TiO_2-CuO (II). The bad

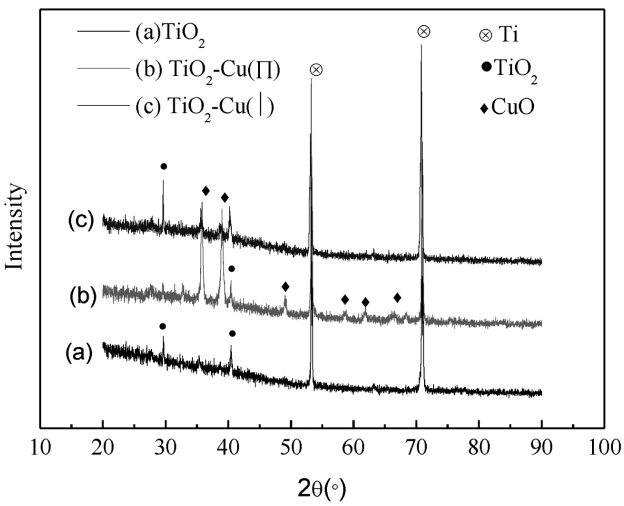

Figure 3: XRD patterns for sintered TiO_2, TiO_2-CuO (I) and TiO_2-CuO (II)

gap was changed dramatically with the increasing CuO amount on the surface of the TiO_2 nanotube arrays. The broad band between 390 nm and 800 nm implies a significant improvement of the absorption in the visible-light region. It can be seen that the adsorption edge of the samples did not shift, which indicates that CuO was deposited onto the TiO_2 nanotube arrays rather than doped into the crystalline TiO_2.[21] The enhanced light adsorption increased the possibilities to separate holes and electrons. Therefore, it can be primarily inferred that the TiO_2-CuO (I) and TiO_2-CuO (II) composites might show a higher photocatalytic performance than the sintered TiO_2 nanotube arrays.

The band-gap energy values (Eg) for different samples were calculated using the following equation: [22]

$$Eg = 1239.89\ m / (-b) \quad (2)$$

The Eg values were 3.25 eV, 3.17 eV and 3.14 eV for the sintered TiO_2, TiO_2-CuO (I) and TiO_2-CuO (II), respectively.

3.4 Photo-electrochemical (PEC) properties

3.4.1 I-V and I-t analysis

The PEC properties of the electrodes were measured by examining their linear-sweep voltammetric profiles in 0.2M Na_2SO_4 in the dark and under illumination. The PEC behavior of the sintered TiO_2, TiO_2-CuO (I) and TiO_2-CuO (II) electrodes exposed to illumination is presented in **Figure 5a**. The current densities in all the photo-electrodes increased with the increasing potential applied to the electrodes, indicating the p-type conductivity. As shown, the maximum current densities of about -4.269×10^{-5} A/cm^2, -4.633×10^{-5} A/cm^2 and -1.1×10^{-5} mA/cm^2 at –0.35 V (vs. SCE) were obtained for the sintered TiO_2, TiO_2-CuO (I) and TiO_2-CuO (II), respectively. TiO_2-CuO (I) exhibits an improved photo-activity compared to the sintered TiO_2 nanotube arrays. However, the TiO_2-CuO (II) sample exhibits a poor photo-activity compared to the sintered TiO_2 nanotube arrays. In the dark area, the maximum photocurrent densities of about -3.367×10^{-5} A/cm^2, -2.29×10^{-5} A/cm^2, -7.908×10^{-6} A/cm^2 at –0.35 V (vs. SCE) were obtained for the sintered TiO_2, TiO_2-CuO (I) and TiO_2-CuO (II), respectively. The sintered TiO_2 exhibits the best electrical behavior of the three samples. And the TiO_2-CuO (II) sample shows the poorest electrical behavior. The results indicate that the bare TiO_2 nanotube arrays modified with CuO through wet impregnation cannot enhance the electron mobility.

A current-time evaluation performed at a fixing bias of –0.2 V vs. SCE for 600 s is shown in **Figure 5b**. The light was continuously chopped with 20-s intervals during the current-time evaluation. **Figure 5c** shows enlarged views of the current-time relationship from the boxed area in **Figure 5b**, corresponding to the whole stages of the current-time measurement of TiO_2-CuO (II). The result indicates that the current density of the sintered TiO_2 and TiO_2-CuO (II) starts to decline immediately after several seconds and remains stable from the 200–300 s measurement to the end of the evaluation. On the other hand, the TiO_2-CuO (I) electrode shows a superior stability under the same evaluation conditions. The current stability of the electrode was quantified as the ratio of the current at the end of the measurement to the current at the beginning of the measurement.[23] The stability of the TiO_2-CuO (I) electrode shows an excellent stability of 95 %. The LSV and current-time results indicate that the growth of the moderate CuO porous film on the TiO_2 nanotube arrays greatly improved the stability of the electrode, although it causes a minor negative effect on the LSV measure-

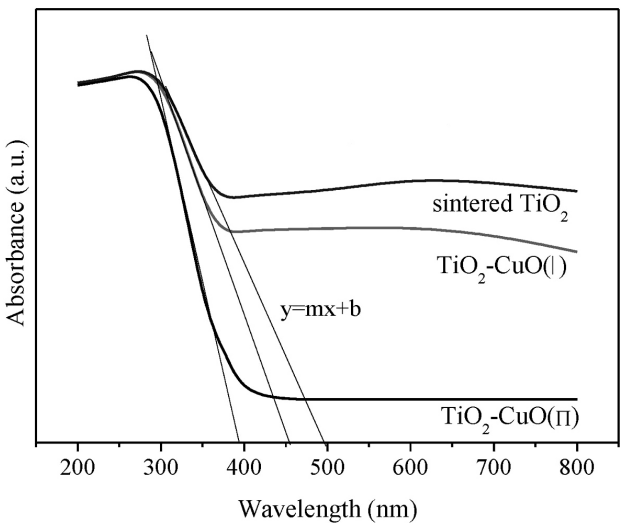

Figure 4: UV-Vis diffuse-reflectance-spectra analysis of sintered TiO_2, TiO_2-CuO (I) and TiO_2-CuO (II); m and b are obtained with the linear fit ($y = m\,x + b$) of the flat section of the UV-Vis spectrum

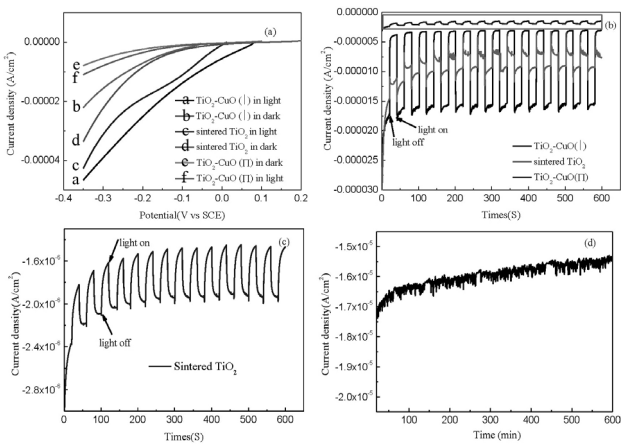

Figure 5: PEC results for the sintered TiO_2, TiO_2-CuO (I) and TiO_2-CuO (II) electrodes: a) electrical-current measurements of the electrodes in the dark and under illumination, b) current-time-measurement results of the sintered TiO_2, TiO_2-CuO (I) and TiO_2-CuO (II) photo-electrodes in the dark and under illumination, c) magnified view of the boxed region from (b); (d) long-time-stability-measurement result for the TiO_2-CuO (I) electrode under illumination

ment by reducing the electrical-current generation. An abundant CuO amount on the TiO_2 nanotube arrays causes a large negative effect on the LSV measurements by reducing the photocurrent generation and electronic transportation. Therefore, it is important to control the CuO content on the surface of TiO_2 nanotube arrays.

During the 6-h reaction process (**Figure 5d**), the photocurrent density over TiO_2-CuO (I) remained vigorous without any obvious deactivation. High efficiency and an excellent current-time stability indicate a great potential of TiO_2-CuO (I) for a wide usage in the hydrogen production. Therefore, drip washing is very important during the wet impregnation followed by sintering.

3.4.2 Electrochemical-impedance-spectroscopy (EIS) analysis

In order to further investigate the effects of the sintered condition and the CuO amount on the PEC performance of TiO_2 nanotube arrays, EIS was performed in a frequency range of 0.01 Hz–100 kHz in 0.2 M of the Na_2SO_4 electrolyte and the results are represented as Nyquist and Bode plots. The EIS measurements were performed on sintered TiO_2, TiO_2-CuO (I) and TiO_2-CuO (II). **Figure 6a** shows the Nyquist plot of the sintered TiO_2, which demonstrates the beginning of a large semicircle usually associated with resistive and capacitive processes. The relationship between Z' (the real part) and Z'' (the imaginary part) of a semicircle with a radius of $R/2$ can be expressed as follows:

$$(Z'-R/2)^2+Z''=(R/2)^2 \quad (3)$$

The relative size of a circular arc radius corresponds to the charge transfer resistance and electron-hole separation efficiency from the Nyquist plot.[24] The Nyquist plots (shown in **Figure 6a**) indicate that the diameter of the semicircle of the sintered TiO_2 under illumination in the high-to-medium frequency region is much smaller than that in the dark.

The relationship between the parallel circuit impedance (Z), resister (R) and capacitor (C) can be expressed as follows:

$$Z=R/(1+\omega CR)-j\omega CR^2/(1+\omega CR^2) \quad (4)$$

As we all know, a low resistance indicates a recombination suppression via an improved charge transport to the electrolyte.[25] The plot of the frequency against the electrochemical impedance of the sintered TiO_2 is shown in **Figure 6b**, indicating that the impedance of the sintered TiO_2 in the dark is about two-fold higher than that under illumination in the low-frequency region. The Nyquist plots in **Figure 6b** show that the diameter of the semicircle of TiO_2-CuO (I) under illumination in the high-to-medium frequency region is much smaller than that in the dark. The plot of the frequency against the electrochemical impedance of the TiO_2-CuO (I) electrode materials is shown in **Figure 6d**. The impedance of the sintered TiO_2-CuO (I) in the dark is about eight-fold higher than that under illumination in the low-frequency region. Moreover, the resistance of the sintered TiO_2 in the dark is lower than that of TiO_2-CuO (I) in the dark according to the analysis from **Figures 6b** and **6d**. In addition, the resistance of the sintered TiO_2 in the dark increases after the CuO loading. Therefore, the electrical activity of the sintered TiO_2 is higher than that of TiO_2-CuO (I), as shown in **Figure 5a**.

The reduction of the TiO_2-CuO (I) resistance under illumination also indicates that CuO might induce a better charge separation and an efficient electron transfer in the TiO_2-CuO. From all the above results, it can be concluded that a moderate amount of CuO provides a way for the hole-electron separation and enhances the photo-electrochemical activity of the electrode. **Figure 6e** shows the Nyquist plot for the TiO_2-CuO (II) electrode. As shown in **Figure 6e**, the diameter of the semicircle of TiO_2-CuO (II) under illumination in the high-to-medium frequency region is smaller than that in

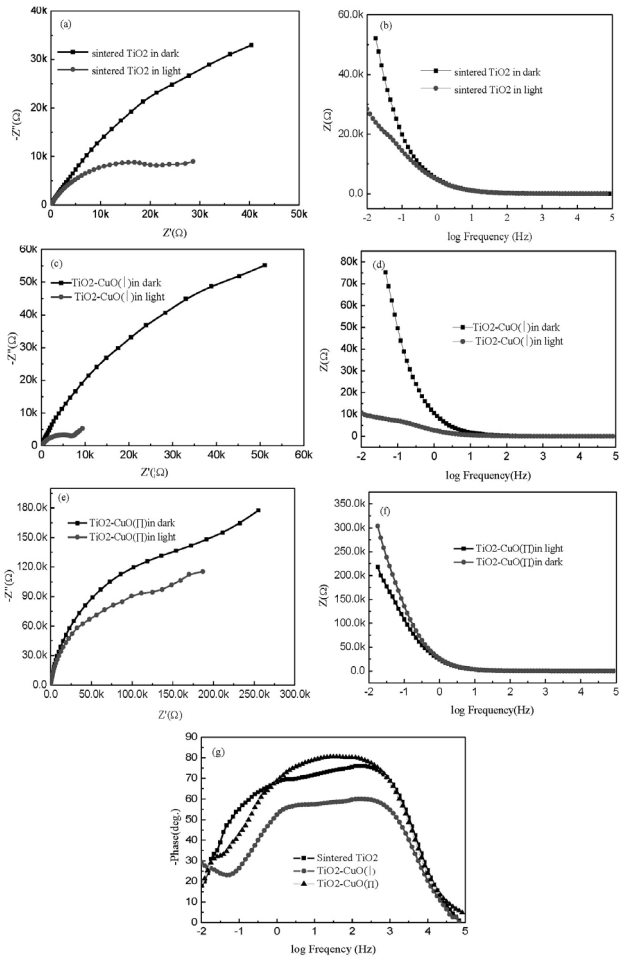

Figure 6: Electrochemical-impedance-spectroscopy results for the sintered TiO_2, TiO_2-CuO (I) and TiO_2-CuO (II) photo-electrodes: a) Nyquist and b) Bode plots obtained for the sintered TiO_2, c) Nyquist and d) Bode plots obtained for TiO_2-CuO (I), e) Nyquist and f) Bode plots obtained for TiO_2-CuO (II), g) Bode phase plot for the sintered TiO_2, TiO_2-CuO (I) and TiO_2-CuO(II) electrodes under illumination

the dark. The plot of frequency against the electrochemical impedance of the TiO_2-CuO (II) photo-electrodes is provided in **Figure 6f**. The impedance of TiO_2-CuO (II) in the dark is about 1.5 times higher than that under illumination in the low-frequency region. The resistance value for the sintered TiO_2 changed significantly after loading a large amount of CuO. And that may be the most important factor contributing to the higher PEC properties of TiO_2-CuO (I) and lower PEC properties of TiO_2-CuO (II).

Furthermore, the Bode plots for the three photo-electrodes (**Figure 6g**) under illumination indicate the presence of time constants at the low- and middle-frequency peaks, corresponding to the diffusion in the electrolyte and the electron transport-recombination process, respectively. The Bode plot for the TiO_2-CuO (I) electrode suggests that the electron transport-recombination process benefited from loading a moderate amount of CuO, thus leading to the highest PEC efficiency of TiO_2-CuO (I). However, the Bode phase plot for the TiO_2-CuO (II) electrode suggests that the electron transport-recombination process did not benefit from an abundant amount of CuO, resulting in the lowest PEC efficiency of the TiO_2-CuO (II) photo-electrode.

3.4.3 Schematic illustration of TiO_2-CuO photo-electrodes

It is well known that combing the p-type photo-electrodes with wide-band-gap n-type semiconductors could not only improve the stability of photo-electrodes, but also enhance the PEC properties due to the formation of a p-n junction. There are many schematic illustrations of p-CuO and n-TiO_2 composites contacting the electrolyte in the thermal-equilibrium state.

Here, our results show that the positive effect of the p–n junction might be suppressed if the thickness of the secondary semiconductor is too high. This is remarkably noticeable when we reckon the CuO with a thick porous sheet layer as a protecting buffer (increasing the resistance). Similar results were observed by A. Kargar[26] and Ulugbek Shaislamov[27] for their p-n PEC electrode, where the thickness of the secondary semiconductor exceeding a certain limit might result in decreasing the PEC performance of photo-electrodes. Moreover, the effect of graphene sheets with various thicknesses on Cu_2O NW electrodes was also reported.[28] High graphene concentrations reduce PEC properties of Cu_2O/graphene electrodes.

The reduced PEC properties of our TiO_2-CuO electrode can be explained based on several influence factors as shown in **Figure 7**: (i) the grain boundaries in the thick porous CuO layer act as recombination sites for the photo-induced electron-hole pairs;[29] (ii) the porous CuO nanosheet layer (including the nanosheet layer and porous CuO shown in **Figure 2b**) leads to additional electrochemical charge-transfer resistance in the dark (shown in **Figure 5**); (iii) the drip washing after WI can

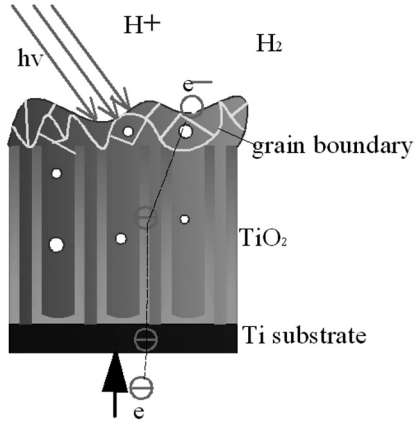

Figure 7: Schematic illustration of the TiO_2-CuO electrode

prevent the formation of large clusters of CuO, acting as the recombination centers resulting in a lower hydrogen-generation activity;[16] and (iv) the CuO layer (shown in **Figure 2c**) on the TiO_2 nanotubes increases the resistance of the electrode in the dark. However, the CuO layer improves the cohesion between CuO and TiO_2, facilitating the charge transfer from TiO_2 to CuO, and resulting in enhancing the proton reduction. These results indicate that the TiO_2-CuO photo-electrode produced through WI by drip washing is more favorable than the TiO_2 electrodes (shown in **Figures 5b** and **5d**) with respect to the long-term stability and PEC performance under photo-electrochemical conditions.

4 CONCLUSIONS

Wet impregnation followed by sintering in air was used to prepare a CuO/TiO_2/Ti heterojunction photo-electrode. High-density porous-nanosheet CuO films on the TiO_2 nanotube arrays (TiO_2-CuO (II)) were obtained without drip washing before sintering, while the CuO films on the TiO_2 nanotube arrays (TiO_2-CuO (I)) were obtained after sintering the sample with drip washing after air drying. Both of the heterojunction photo-electrodes extend the absorption of visible light. It was found that the CuO growth could significantly reduce the PEC properties of a photo-electrode due to the additional electrochemical charge-transfer resistance. The photocatalytic stability of TiO_2 was remarkably enhanced up to 95 % because of the formation of CuO/TiO_2 interfaces due to the drip washing during the preparation. The EIS measurement indicates that an abundant amount of CuO on the TiO_2 nanotube arrays could increase the electric resistance, resulting in decreasing the photocurrent density during the LSV test. The fabricated TiO_2/CuO photo-electrode exhibited an excellent electrochemical stability, which is highly favorable, having a great potential for the application of other unstable metal-oxide semiconductor-based electrodes.

Acknowledgments

This work was supported by the Zhejiang Province Science Foundation for Youths (No. LQ16E020002). The work of material characterization was supported by the Zhejiang Metallurgical Research Institute Co., Ltd.

5 REFERENCES

[1] T. W. Kim, K.-S. Choi, Nanoporous BiVO4 photoanodes with dual-layer oxygen evolution catalysts for solar water splitting, Science, 334 (**2014**), 990–994, doi: 10.1126/science.1246913

[2] Y. W. Phuan, M. N. Chong, J. D. Ocon, E. S. Chan, A novel ternary nanostructured carbonaceous-metal-semiconductor eRGO/NiO/α-Fe_2O_3 heterojunction photoanode with enhanced charge transfer properties for photoelectrochemical water splitting, Solar Energy Materials and Solar Cells, 169 (**2017**), 236–244, doi:10.1016/j.solmat.2017.05.028

[3] A. Subramanian, Z. Pan, H. Li, L. Zhou, W. Li, Y. Qiu, Y. Xu, Y. Hou, C. Muzi, Y. Zhang, Synergistic promotion of photoelectrochemical water splitting efficiency of TiO2 nanorods using metal-semiconducting nanoparticles, Applied Surface Science, 430 (**2017**), 621–637, doi:10.1016/j.apsusc.2017.05.190

[4] S. Bagheri, Z. A. M. Hir, A. T. Yousefi, S. B. A. Hamid, Progress on mesoporous titanium dioxide: Synthesis, modification and applications, Microporous and Mesoporous Materials, 218 (**2015**), 206–222, doi:10.1016/j.micromeso.2015.05.028

[5] V. C. Anitha, A. N. Banerjee, S. W. Joo, Recent developments in TiO2 as n- and p- type transparent semiconductors: synthesis, modification, properties, and energy-related applications, Journal of Materials Science, 50 (**2015**), 7495–7536, doi:10.1007/s10853-015-9303-7

[6] H. Fu, X. Yang, X. An, W. Fan, X. Jiang, A. Yu, Experimental and theoretical studies of V_2O_5@TiO_2 core-shell hybrid composites with high gas sensing performance towards ammonia, Sensors and Actuators B: Chemical, 252 (**2017**), 103–115, doi:10.1016/j.snb.2017.05.027

[7] A. H. Mamaghani, F. Haghighat, C.-S. Lee, Photocatalytic oxidation technology for indoor environment air purification: The state-of-the-art, Applied Catalysis B: Environmental, 203 (**2017**), 247–269, doi: 10.1016/j.apcatb.2016.10.037

[8] M. Ni, M. K. H. Leung, D. Y. C. Leung, K. Sumathy, A review and recent developments in photocatalytic water-splitting using TiO2 for hydrogen production, Renew Sust Energ Rev, 11 (**2007**), 401–425, doi: 10.1016/j.rser.2005.01.009

[9] M. Wang, J. Ioccozia, L. Sun, C. Lin, Z. Lin, Inorganic-modified semiconductor TiO_2 nanotube arrays for photocatalysis, Energy Environmental Science, 7 (**2014**), 2182–2202, doi:10.1039/C4EE00147H

[10] J. Lv, H. Gao, H. Wang, X. Lu, G. Xu, D. Wang, Z. Chen, X. Zhang, Z. Zheng, Y. Wu, Controlled deposition and enhanced visible light photocatalytic performance of Pt-modified TiO_2 nanotube arrays, Applied Surface Science, 351 (**2015**), 225–231, doi:10.1016/j.apsusc.2015.05.139

[11] X. Fan, J. Fan, X. Hu, E. Liu, L. Kang, C. Tang, Y. Ma, H. Wu, Y. Li, Preparation and characterization of Ag deposited and Fe doped TiO_2 nanotube arrays for photocatalytic hydrogen production by water splitting, Ceramics International, 40 (**2014**), 15907–15917, doi:10.1016/j.ceramint.2014.07.119

[12] X. Lu, X. Li, J. Qian, N. Miao, C. Yao, Z. Chen, Synthesis and characterization of CeO_2/TiO_2 nanotube arrays and enhanced photocatalytic oxidative desulfurization performance, Journal of Alloys and Compounds, 661 (**2016**), 363–371, doi:10.1016/j.jallcom.2015.11.148

[13] M. Santamaria, G. Conigliaro, F. Di Franco, F. Di Quarto, Photoelectrochemical Evidence of Cu_2O/TiO_2 Nanotubes Hetero-Junctions Formation and their Physicochemical Characterization, Electrochimica Acta, 144 (**2014**), 315–323, doi:10.1016/j.electacta.2014.07.154

[14] Y. J. Wang, M. Yang, L. Z. Ren, W. Q. Zhou, K. G. Yang, F. M. Yu, M. Meng, S. X. Wu, S. W. Li, Enhanced Raman Scattering in Copper-Doped TiO_2 films, Thin Solid Films, 598 (**2016**), 311–314, doi: 10.1016/j.tsf.2015.12.036

[15] M. Tripathi, P. Chawla, Optimization of semiconductor ns-TiO_2-CuO admixed photoelectrode for photoelectrochemical solar cell in regard to hydrogen production, International Journal of Hydrogen Energy, 41 (**2016**), 7993–7996, doi:10.1016/j.ijhydene.2015.11.163

[16] S. Xu, A. J. Du, J. Liu, J. Ng, D. D. Sun, Highly efficient CuO incorporated TiO_2 nanotube photocatalyst for hydrogen production from water, International Journal of Hydrogen Energy, 36 (**2011**), 6560–6568, doi: 10.1016/j.ijhydene.2011.02.103

[17] S. Han, J. Li, X. Chen, Y. Huang, C. Liu, Y. Yang, W. Li, Enhancing photoelectrochemical activity of nanocrystalline WO3 electrodes by surface tuning with Fe(iii), International Journal of Hydrogen Energy, 37 (**2012**), 16810–16816, doi:10.1016/j.ijhydene.2012.08.145

[18] H. Cao, Z. Fan, G. Hou, Y. Tang, G. Zheng, Ball-flower-shaped Ni nanoparticles on Cu modified TiO_2 nanotubearrays for electrocatalytic oxidation of methanol, Electrochimica Acta, 125 (**2014**), 275–281, doi:10.1016/j.electacta.2014.01.101

[19] L. De Los Santos Valladares, D. Hurtado Salinas, A. Bustamante Dominguez, D. Acosta Najarro, S. I. Khondaker, T. Mitrelias, C. H. W. Barnes, J. Albino Aguiar, Y. Majima, Crystallization and electrical resistivity of Cu_2O and CuO obtained by thermal oxidation of Cu thin films on SiO_2/Si substrates, Thin Solid Films, 520 (**2012**), 6368–6374, doi:10.1016/j.tsf.2012.06.043

[20] M. A. Abdel-Rahim, M. A. S. Hammam, A. A. Abu-Sehly, M. M. Hafiz, Composition effect on the pre-crystallization and crystallization characteristics for Se90-xTe10Agx, Journal of Alloys and Compounds, 728 (**2017**), 1346–1361, doi:10.1016/j.jallcom.2017.09.004

[21] Y.-H. Yu, Y.-P. Chen, Z. Cheng, Microwave-assisted synthesis of rod-like CuO/TiO_2 for high-efficiency photocatalytic hydrogen evolution, International Journal of Hydrogen Energy, 40 (**2015**), 15994–16000, doi:10.1016/j.ijhydene.2015.09.115

[22] R. López, R. Gómez, Band-gap energy estimation from diffuse reflectance measurements on sol-gel and commercial TiO_2: a comparative study, Journal of Sol-Gel Science and Technology, 61 (**2012**), 1–7, doi: 10.1007/s10971-011-2582-9

[23] Q. Huang, F. Kang, H. Liu, Q. Li, X. Xiao, Highly aligned Cu_2O/CuO/TiO_2core/shell nanowire arrays as photocathodes for water photoelectrolysis, Journal of Materials Chemistry A, 1 (**2013**), 2418–2425, doi:10.1039/C2TA00918H

[24] W. H. Leng, Z. Zhang, J. Q. Zhang, C. N. Cao, Investigation of the Kinetics of a TiO_2 Photoelectrocatalytic Reaction Involving Charge Transfer and Recombination through Surface States by Electrochemical Impedance Spectroscopy, Journal of Physical Chemistry B, 109 (**2005**) 31, 15008–15023, doi: 10.1021/jp051821z

[25] T. Lopes, L. Andrade, H. A. Ribeiro, A. Mendes, Characterization of photoelectrochemical cells for water splitting by electrochemical impedance spectroscopy, International Journal of Hydrogen Energy, 35 (**2010**), 11601–11608, doi: 10.1016/j.ijhydene.2010.04.001

[26] A. Kargar, Y. Jing, S. J. Kim, C. T. Riley, X. Pan, D. Wang, ZnO/CuO heterojunction branched nanowires for photoelectrochemical hydrogen generation, ACS Nano, 7 (**2013**), 11112–11120, doi:10.1021/nn404838n

[27] U. Shaislamov, K. Krishnamoorthy, S. J. Kim, A. Abidov, B. Allabergenov, S. Kim, S. Choi, R. Suresh, W. M. Ahmed, H.-J. Lee, Highly stable hierarchical p-CuO/ZnO nanorod/nanobranch photoelectrode for efficient solar energy conversion, International Journal of Hydrogen Energy, 41 (**2016**), 2253–2262, doi:10.1016/j.ijhydene.2016.01.168

[28] A. A. Dubale, W.-N. Su, A. G. Tamirat, C.-J. Pan, B. A. Aragaw, H.-M. Chen et al., The synergetic effect of graphene on Cu_2O nanowire arrays as a highly efficient hydrogen evolution photocathode in water splitting, Journal of Materials Chemistry A, 2 (**2014**), 18383–18397, doi:10.1039/C4TA03464C

[29] Y. Park, W. Kim, D. Monllor-Satoca, T. Tachikawa, T. Majima, W. Choi, Role of interparticle charge transfers in agglomerated photocatalyst nanoparticles: demonstration in aqueous suspension of dye-sensitized TiO_2, Journal of Physical Chemistry Letters, 4 (**2013**), 189–194, doi:10.1021/jz301881d